Theoretical analysis of transmission error in rack and pinion systems

Ibai Ulacia[1,*], *Miryam B.* Sánchez[2], *Aurea* Iñurritegui[1], *Aitor* Arana[1], *Jon* Larrañaga[1], and *José I.* Pedrero[2]

[1]Mondragon Unibertsitatea, Faculty of Engineering, Loramendi 4, 20500 Mondragon, Spain
[2]UNED, Departamento de Mecánica, Juan del Rosal 12, 28040 Madrid, Spain

Abstract. Rack and pinion drive systems are widely used in machine tools with long travel distances because the stiffness is independent of the travelled distance, in contrast to other drive systems such as ballscrews. Although the inherent backlash problem of gear systems has been solved by means of utilizing two pinions independently preloaded, the time-varying mesh stiffness causes periodic position differences between the motor encoder and table position, which is known as transmission error, and may lead to vibrations and dynamic load. Few experimental works have analyzed such transmission error, but there are no theoretical approaches in the scientific literature. Therefore, this work aims to first extend previous analytical and approximate equations for mesh stiffness of gearing to rack and pinion systems and validate them with finite element methods. Finally, the effect of geometry variations, such as pressure angle and tooth thickness tolerance, on transmission error is discussed.

1 Introduction

Rack and pinion drive systems are widely employed in machine tools with long travel distances due to their inherent advantages, including high stiffness and independence from the travelled distance. Unlike other drive systems, such as ballscrews, where stiffness can vary based on the distance travelled, rack and pinion systems provide consistent stiffness throughout the entire travel range [1]. This characteristic makes them particularly suitable for applications requiring precise and rigid positioning.

However, despite the advantages of rack and pinion systems, they are not immune to certain challenges. One significant issue is the presence of backlash inherent to any geared system. To mitigate such source errors, one notable approach involves the utilization of two pinions with independent preload, which effectively addresses the inherent backlash problem in gear systems [2, 3]. By independently preloading the pinions, the inherent backlash can be minimized, ensuring a more precise and reliable operation of the rack and pinion drive system [4].

Another significant issue is the transmission error, which refers to periodic position differences between the motor encoder and the table position during operation. Transmission error occur due to the time-varying mesh stiffness inherent in gear systems [5-9]. These periodic position differences, if not properly controlled, can lead to detrimental effects such as dynamic load, vibrations, and reduced positioning accuracy, impacting the overall performance of the system.

While some experimental works have explored the analysis of transmission error in rack and pinion systems [10], there is a significant gap in the existing literature when it comes to theoretical approaches. The few theoretical approaches in rack and pinion systems are related to other applications, such as pure rolling [11], automotive engine [12], and steering rack [13] or ship lift mechanism [14], but they are not focused on transmission error. The scientific literature lacks comprehensive theoretical investigations and models specifically addressing transmission error in rack and pinion systems. Therefore, there is a need to develop analytical and approximate equations to accurately quantify the mesh stiffness of gearing in rack and pinion systems.

The objective of this research is to bridge this gap and provide a theoretical analysis of transmission error in rack and pinion systems. The primary aim is to extend previous analytical and approximate equations for mesh stiffness of gearing to specifically address rack and pinion systems. These equations will be validated through finite element methods, ensuring the accuracy and reliability of the theoretical model. Furthermore, the research will explore the effect of geometry variations, such as pressure angle and tooth thickness tolerance, on transmission error, shedding light on potential strategies for mitigating this issue.

By conducting a comprehensive theoretical analysis, this research contributes to the understanding and optimization of rack and pinion drive systems, leading to enhanced performance, reduced vibrations, and improved positioning accuracy. The findings of this study will provide valuable insights for engineers and researchers involved in the design, development, and control of machine tools and other applications utilizing rack and pinion systems.

* Corresponding author: iulacia@mondragon.edu

2 Analytical model for the mesh stiffness

The mesh stiffness of a tooth pair, also called single mesh stiffness (SMS) and denoted by K_M, can be expressed as [5]:

$$K_M = \left(\frac{1}{k_{x1}}+\frac{1}{k_{s1}}+\frac{1}{k_{n1}}+\frac{1}{k_{R1}}+\frac{1}{k_{x2}}+\frac{1}{k_{s2}}+\frac{1}{k_{n2}}+\frac{1}{k_{R2}}+\frac{1}{k_H}\right)^{-1} \quad (1)$$

where k_x is the bending stiffness, k_s the shear stiffness, k_n the compressive stiffness, k_R the gear body stiffness, k_H the contact stiffness, and subscripts 1 and 2 denote the pinion and the rack, respectively.

The bending, shear, and compressive stiffnesses can be assessed from the potential energy method, which is a widely accepted analytical approach [5]. This method treats the gear tooth as a variable-section cantilever beam fixed at its dedendum diameter and estimates its total potential energy by solving analytical expressions derived from mechanics of materials. Accordingly, the equations for three components are:

$$\frac{1}{k_x} = \frac{12}{Eb}\int_{y_p}^{y_C}\left[(y_C - y)\cos\alpha_C - r_c \sin\frac{\gamma_c}{2}\sin\alpha_C\right]^2 \frac{\mathrm{d}\,y}{e^3(y)} \quad (2)$$

$$\frac{1}{k_n} = \frac{1}{Eb}\int_{y_p}^{y_C}\sin^2\alpha_C\,\frac{\mathrm{d}\,y}{e(y)} \quad (3)$$

$$\frac{1}{k_s} = C_s\frac{1}{Gb}\int_{y_p}^{y_C}\cos^2\alpha_C\,\frac{\mathrm{d}\,y}{e(y)} \quad (4)$$

where E is the modulus of elasticity of steel, G is the transverse modulus of elasticity, b is the face width, and C_s is the shear stress correction factor, which for a rectangular section takes the value $C_s = 1.2$. Subscript c denotes the contact point and therefore r_c is the radius of the contact point, γ_c the angular thickness at the corresponding tooth section, and α_C the load angle at this contact point. Finally, y is a linear coordinate along the tooth centerline from the center of the gear (gear rotation axis), y_p corresponds to the embedded tooth section at the dedendum circle, y_c corresponds to the load tooth section, and $e(y)$ is the chordal thickness at tooth section described by y. For the tooth rack, the origin of coordinate y is an arbitrary plane parallel to the pitch plane, the angular thicknesses are equal to the corresponding chordal thicknesses, and the load angle is equal to the standard normal pressure angle α_n at any contact point.

The contact stiffness can be assessed from the Hertz approach or Weber-Banaschek approach. The Hertz approach results in [5]:

$$k_H^{-1} = \frac{4}{\pi}\frac{1-\nu^2}{Eb} \quad (5)$$

ν being the Poisson ratio. The Weber approach is more complicated and can be found in [6]. Finally, the gear body stiffness can be calculated according to Weber-Banaschek [6] or Sainsot [7] contributions.

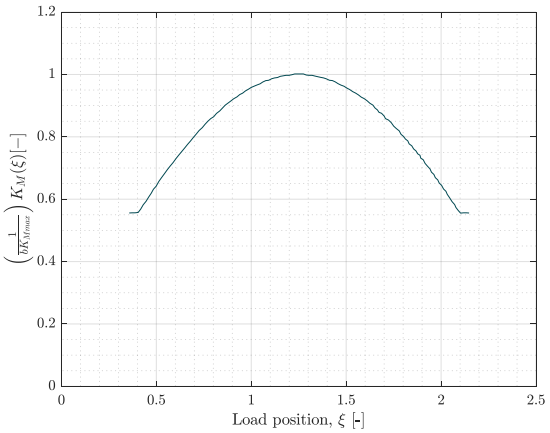

Fig. 1. Typical shape of single mesh stiffness curve.

Different combinations of those approaches were studied in [8], but in all the cases the curve of single mesh stiffness presents a shape as the one in Figure 1.

This curve can be accurately approximated by the equation [5]:

$$K_M(\xi) = K_{Mmax}\cos\left(b_0(\xi - \xi_m)\right) \quad (6)$$

where K_{Mmax} is the SMS at the midpoint of the path of contact, subscript m denotes this midpoint, and:

$$b_0 = \left[\frac{1}{2}\left(\kappa_1 + \frac{\varepsilon_\alpha}{2}\right)^2 - \kappa_2\right]^{-1/2} \quad (7)$$

$$\xi = \frac{z_1}{2\pi}\sqrt{\frac{r_{c1}^2}{r_{b1}^2} - 1} \quad (8)$$

in which ε_α in the contact ratio, z_1 the number of teeth on pinion, and r_b the base radius. Coefficients κ_1 and κ_2 are introduced to adjust the SMS curve to eq. (6). Values for κ_1 and κ_2 for different combinations of contact stiffness and gear body stiffness can be found in [8]. In all the cases, the value of K_{Mmax} should be obtained from numerical calculations or FE analyses. Obviously, K_{Mmax} depends on the geometry of the meshing gears and the specific considered combination of approaches, but not on the applied torque.

It is observed that the rotation of the pinion $\Delta\vartheta$ is related with the parameter ξ as follows:

$$\Delta\vartheta = \frac{2\pi}{z_1}\Delta\xi \quad (9)$$

3 Finite element model

A quasi-static two-dimensional finite element model (FEM) is developed to analyze and assess the impact of transmission error in rack and pinion systems. The numerical models are automatically generated using a specialized gear mesh generator [15], and the FEM models are computed using *Abaqus* solver.

The generation of rack and pinion mesh follows the well-stablished methodology introduced by Litvin [16]. This methodology entails assigning a higher density of elements to the teeth compared to the body of the pinion,

as depicted in Figure 2. Additionally, a progressive mesh density, known as bias factor, is determined from the symmetry axis of the tooth to the contact area [17]. To accurately capture the behavior of the system, four-node, isoparametric, arbitrary quadrilateral elements suitable for plane stress applications are employed (specifically, element type CPS4 in the *Abaqus* software [18]).

Regarding the boundary conditions, a prescribed translation velocity is imposed on the rack (v) to simulate fixed linear motion, while a torque (T) is applied to the pinion. To mitigate the influence of boundary conditions, all the teeth of the pinion are taken into consideration in the simulations [19]. Moreover, in order to avoid preloading of the teeth during contact initiation, a preliminary interference was introduced between meshing teeth. It induces a small angular deviation ϑ_0, which should be accounted for comparisons between FEM and analytical models.

The transmission error $TE(\vartheta)$ is determined by calculating the difference between the computed rotation of the pinion ϑ_P^{FEM} and the theoretical rotation resulting from the prescribed translation of the rack ϑ_P^T, as described in eq. (10). This calculation allows for the quantification of the deviation or variation between the actual motion of the pinion and the expected motion based on the translation of the rack, accounting for the deformations arising from mesh stiffness.

$$TE(\vartheta) = \vartheta_P^{FEM} - \vartheta_P^T \tag{10}$$

where:

$$\vartheta_P^T = \frac{v \cdot t}{\pi \cdot m_n \cdot z_1} \tag{11}$$

Here, t represents the simulated time (with a time increment employed of 1 ms in this specific case), and m_n denotes the normal module.

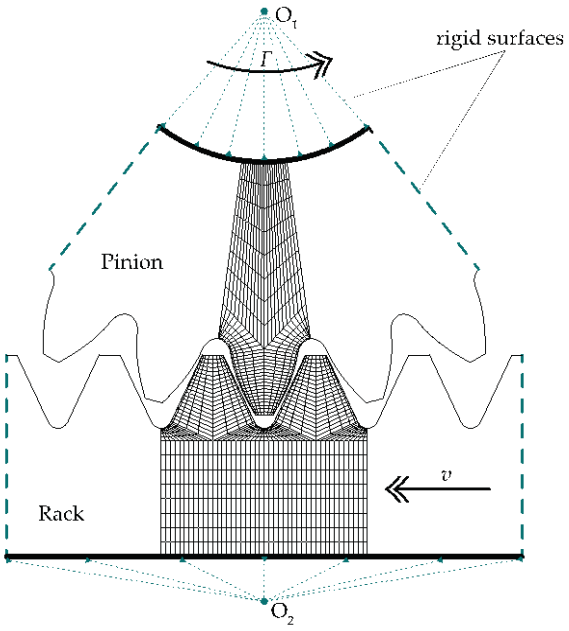

Fig. 2. Finite element mesh detail and boundary conditions of the numerical model.

4 Approximate equations for the time-varying mesh stiffness and transmission error

From the hypothesis of minimum elastic potential energy, the theoretical load at a specific tooth pair F_i at the load position described by ξ is [5]:

$$F_i(\xi) = \frac{K_{Mi}(\xi)}{\sum_j K_{Mj}(\xi)} F_T = \frac{K_{Mi}(\xi)}{\sum_j K_M(\xi + j)} F_T \tag{12}$$

where F_T is the total transmitted load and the sum is extended to all the tooth-pairs in simultaneous contact.

Accordingly, the theoretical tooth-pair deflection δ_i at any contact position will be given by [5]:

$$\delta_i(\xi) = \frac{F_i(\xi)}{K_{Mi}(\xi)} = \frac{F_T}{\sum_j K_M(\xi + j)} \tag{13}$$

As the right term does not depend on i, the tooth pair deflection is equal for all the tooth-pairs in contact and describes the delay of the driven gear with respect to the driving gear, as a distance measured on the pressure line. Obviously, the relation between the delay distance and the angle transmission error is:

$$TE(\xi) = \frac{\delta(\xi)}{r_{b1}} = \frac{F_T}{r_{b1}} \frac{1}{\sum_j K_M(\xi + j)} \tag{14}$$

$$TE(\vartheta) = \frac{F_T}{r_{b1}} \frac{1}{\sum_j K_M\left(\frac{z_1}{2\pi}\xi - \vartheta_0 + j\right)} \tag{15}$$

Equations (12) to (15) correspond to the theoretical contact model and are valid for weakly loaded teeth. For heavily loaded teeth, the delay of the driven gear results in an earlier start of contact and a delayed end of contact [20]. These additional contact intervals depend on the transmitted load and result in an affective contact ratio greater than the theoretical one. As described in [20], the distance δ_G that the driving tooth should approach to (or move away) the driven one to start (end) the contact at a given meshing position ξ, can be expressed as:

$$\delta_G(\xi) = \left(\frac{2\pi}{Z_1}\right)^2 C_{p-inn}\, r_{b1} (\xi_{inn} - \xi)^2 \tag{16}$$

$$\delta_G(\xi) = \left(\frac{2\pi}{Z_1}\right)^2 C_{p-out}\, r_{b1} (\xi - \xi_{out})^2 \tag{17}$$

where ξ_{inn} and ξ_{out} are the inner and outer limits of the theoretical contact interval, and C_{p-inn} and C_{p-out} can be computed as described in [20]. Accordingly, considering that $\delta_G(\xi) = 0$ inside the theoretical contact interval, the load transmitted by the tooth pair is:

$$F(\xi) = K_M(\xi)\big(\delta(\xi) - \delta_G(\xi)\big) \tag{18}$$

the total transmitted load will be:

$$\begin{aligned} F_T &= \sum_j K_M(\xi + j)\big(\delta(\xi) - \delta_G(\xi + j)\big) \\ &= \delta(\xi) \sum_j K_M(\xi + j) - \sum_j K_M(\xi + j)\delta_G(\xi + j) \end{aligned} \tag{19}$$

and the tooth-pair deflection:

$$\delta(\xi) = \frac{F_T + \sum_j K_M(\xi + j)\delta_G(\xi + j)}{\sum_j K_M(\xi + j)} \quad (20)$$

from which the transmission error will be given by:

$$TE(\xi) = \frac{F_T + \sum_j K_M(\xi + j)\delta_G(\xi + j)}{r_{b1}\sum_j K_M(\xi + j)} \quad (21)$$

Finally, the time varying meshing stiffness can be expressed as:

$$K_T(\xi) = \frac{F_T}{\delta(\xi)} \quad (22)$$

Equations (18), (21), and (22) describe the evolution of the load sharing, transmission error, and meshing stiffness along the path of contact under actual load conditions. The limits of the actual contact interval (extended contact interval), $\xi_{\min}$ and $\xi_{\max}$, can be obtained from eq. (18), by doing $F(\xi) = 0$. The actual contact ratio will be given by:

$$\varepsilon_{\alpha-ext} = \xi_{\max} - \xi_{\min} \quad (23)$$

5 Results and discussion

5.1. Case studies

Table 1 summarizes the geometrical characteristics of the rack and pinion system under consideration. Five different torque levels are applied, ranging from 50 Nm to 150 Nm. The material selected for the pinion and rack is a steel with 206 GPa Young modulus and 0.3 Poisson coefficient.

Three case studies have been selected with the aim of validating the proposed model for rack and pinion systems. The theoretical contact ratio of each case is respectively, 1.657, 1.791 and 1,657. First, Case 2 focuses on studying the effect of pressure angle on the transmission error, aiming to observe the effect of the contact ratio. Subsequently, Case 3 introduces the influence of tooth thickness tolerance, serving to demonstrate the capability of the proposed model in accommodating tooth geometry modifications.

5.2. Model validation

To apply the extended contact model to the contact in rack-pinion systems, it is necessary to adjust the coefficients κ_1 and κ_2 of the single mesh stiffness curve (eqs. (6) and (7)). As the flexibility of the gear body affects the SMS, the coefficients κ_1 and κ_2 will be influenced by the pinion rim thickness and pinion size. It has been proved that κ_1 and κ_2 for internal and external gears are different, even for the same approaches of the contact and gear body stiffnesses [21]. In addition, analytical approaches of Weber [6] and Sainsot [7] are not valid for very high number of teeth, as frequently occurs for internal gears, and even more for infinite teeth, as the rack case.

After a correlation study, the adjusted values of the coefficients κ_1 and κ_2 for rigid body tooth pinion and rack body height around 1.5 m_n are the following:

$$\kappa_1 = 1.661 \quad (24)$$

$$\kappa_2 = 2.233 \quad (25)$$

These values are not far from those of rigid body pinion and wheel (approach IV in [8]) where $\kappa_1 = 1.56$ and $\kappa_2 = 2.00$, indicating a reasonable result.

Moreover, the SMS at the midpoint of the path of contact (K_{Mmax}) has been calculated through FEM analysis for the three cases, with stiffness units expressed in N/mm:

$$K^1_{Mmax} = 5.076 \cdot 10^5 \quad (26)$$

$$K^2_{Mmax} = 4.814 \cdot 10^5 \quad (27)$$

$$K^3_{Mmax} = 4.784 \cdot 10^5 \quad (28)$$

These values are consistent with other findings in the literature for similar gear geometries [22] and capture the distinctive variations among the case studies. Specifically, the first case exhibits the highest stiffness due to a higher pressure angle, whereas the last case displays the lowest stiffness due to a smaller tooth root thickness.

Upon calculating the specific coefficients for the proposed analytical model (eq. 24-28), a comparison between the analytical model and Finite Element Method (FEM) results is presented in Figure 3. It is important to note that the coordinate system of the FEM curves has been adjusted to align with the analytical curves, compensating for the initial offset introduced in the FEM during contact initiation.

The results reveal that the proposed approximate model accurately represents both the overall values and the shape of the transmission error in rack and pinion systems. The model effectively captures the characteristics of the single tooth contact region and the contact ratio. Furthermore, the peak-to-peak error, which contributes to the dynamic load, exhibits a strong correlation between the analytical model and the numerical FEM, with maximum error lower than 5% for all the analyzed cases, as depicted in Figure 4.

Table 1. Geometry parameters of the rack and pinion system.

	Symbol	Case 1	Case 2	Case 3
Number of teeth	z_1	24		
Normal module	m_n	2.116 mm		
Pressure angle	α_n	22.5°	20º	22.5º
Face width	b	25 mm		
Profile shift	x_1	0		
Operating center distance	a_w	25.392 mm		
Reference profile - ISO 53	[-]	A (1.25/0.25/0.38)		
Tolerance - DIN 3967	[-]	0	0	- 90 μm

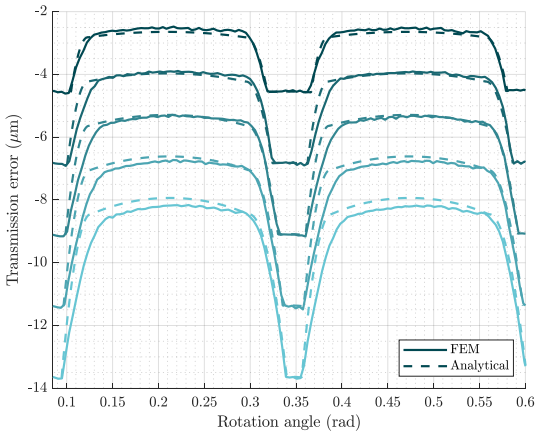

Fig. 3. Transmission error results for the FEM (continuous line) and analytical model (discontinuous line) for Case 1.

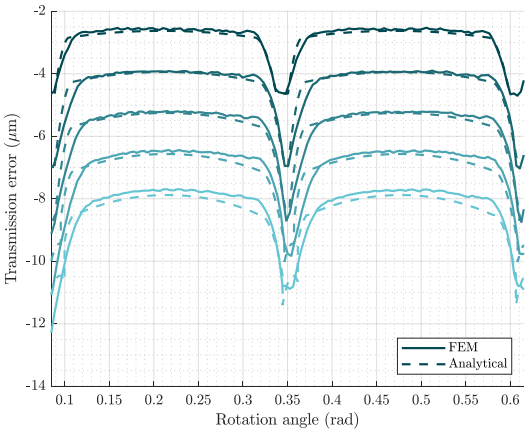

Fig. 5. Transmission error results for the FEM (continuous line) and analytical model (discontinuous line) for Case 2.

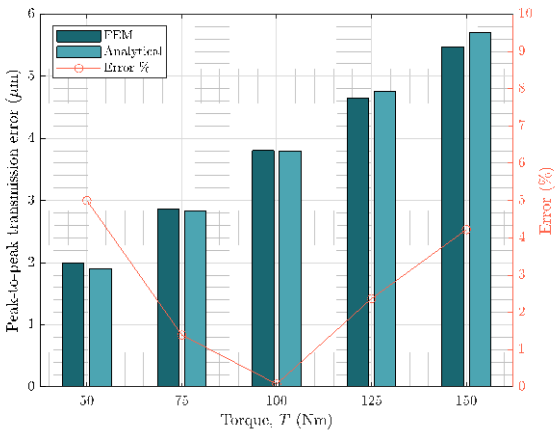

Fig. 4. Peak-to-peak transmission error for different torque and maximum error between analytical and FEM results for Case 1.

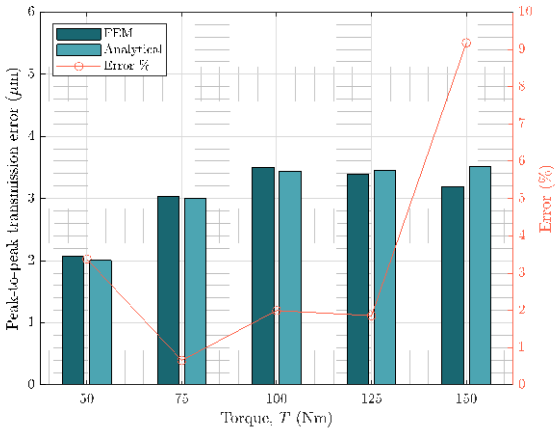

Fig. 6. Peak-to-peak transmission error for different torque and maximum error between analytical and FEM results for Case 2.

Looking into the differences, it can be observed that the analytical model predicts a symmetrical response in the transmission error, whereas the FEM results exhibit a different response during the loading and unloading phases from single to double teeth contact regions. These findings are in agreement with the results reported in [22], where an increase in such asymmetry was observed when increasing the transmission ratio. In the context of rack and pinion systems, where the transmission ratio is theoretically infinite, this represents the extreme condition and that is why it is even more noticeable. However, it is worth noting that for practical applications, these differences can be considered negligible, even under such extreme transmission ratio conditions.

5.3. Influence of the pressure angle

Following the validation of the analytical model, an investigation into the impact of the pressure angle is conducted. The pressure angle influences the amplitude of SMS and the contact ratio, which results in a slightly different curves of mesh stiffness and transmission error. The results for a pressure angle of 20° are presented in Figure 5. Notably, both models exhibit remarkably similar results, with peak-to-peak transmission error values consistently below 10% (as illustrated in Figure 6).

Furthermore, when compared to case study 1, it is worth noting that the initial peak-to-peak transmission error exhibits a slight increase, which aligns with the expected trend attributed to lower stiffness values. However, it is also noticeable that the contact ratio is higher in this case study, resulting in a shorter single tooth contact region. Consequently, for torques exceeding 100 Nm, three teeth come into contact, leading to the stabilization of the peak-to-peak transmission error. Both models successfully capture this phenomenon, although some discrepancies are observed within these regions. Probably, the FEM model is slightly less accurate for three tooth-pairs in contact; however, discrepancies are small, and results can be considered acceptable.

5.4. Influence of thickness tolerance

Finally, the effect of tooth thickness is considered in the analysis. Figure 7 shows the comparison between analytical and FEM results for the transmission error, while Figure 8 depicts the corresponding peak-to-peak transmission error. Notably, the obtained results align with previous findings, demonstrating a strong agreement between both models. When comparing it to Case 1, the stiffness of the tooth is lower and therefore, slight increase of the peak-to-peak transmission errors are observed.

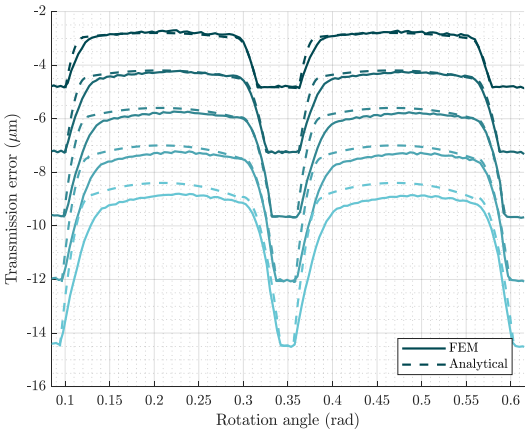

Fig. 7. Transmission error results for the FEM (continuous line) and analytical model (discontinuous line) for Case 3.

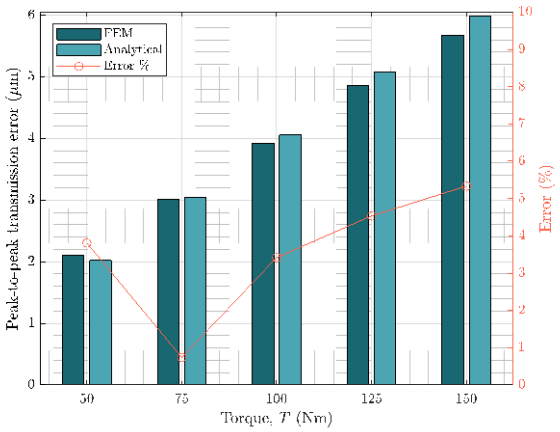

Fig. 8. Peak-to-peak transmission error for different torque and maximum error between analytical and FEM results for Case 3.

6 Conclusions

Based on the results shown in the present study, the following conclusions can be drawn:

- The proposed analytical model effectively represents the transmission error in rack and pinion systems, capturing both the overall values and the shape of the transmission error curve.
- The effect of different factors on the transmission error has been investigated. The impact of variables such as pressure angle, tooth thickness, and contact ratio has been examined. The results demonstrate that these factors influence the magnitude and characteristics of the transmission error.
- The analysis of the transmission error under different scenarios and conditions provides valuable insights for understanding the dynamic behavior and performance of rack and pinion systems. These findings contribute to improving the design and operational efficiency of these systems.

In conclusion, the results highlight the accuracy of the analytical model, the influence of various factors on the transmission error, and the significance of tooth stiffness. This knowledge enhances our understanding of rack and pinion systems and enables informed decision-making for design improvements and performance optimization.

Acknowledgements

The authors express their gratitude to the Spanish Council for Scientific and Technological Research for the support of the project PID2019-110996RB-I00, and UNED for the support of the action 2023-ETSII-UNED-04. I. Ulacia is also grateful to the Basque Government´s Department of Education for the support of the project ref. MV_2023_1_0033.

References

1. L. Uriarte, M. Zatarain, D. Axinte, J. Yagüe-Fabra, S. Ihlenfeldt, J. Eguia, A. Olarra, CIRP Ann. **62** (2013)
2. A. Verl, T. Engelberth, CIRP Ann. **67** (2008)
3. T. Engelbert, S. Apprich, J. Friedrich, D. Coupek, A. Lechler, Prod. Eng. Res. Devel. **9** (2015)
4. O. Franco, X. Beudaert, K. Erkorkmaz, J. Manuf. Mater. Process. **4** (2020)
5. M.B. Sánchez, M. Pleguezuelos, J.I. Pedrero, Mech. Mach. Theory **109** (2017)
6. C. Weber, K. Banaschek, Vieweg Verlag, Braunschweig, Germany (1955)
7. P. Sainsot, P. Velex, O. Duverger, J. Mech. Des. **126** (2004)
8. M. Pleguezuelos, M.B. Sánchez, J.I. Pedrero, MATEC web of Conferences **317** (2020)
9. J. Marafona, P. Marques, R. Martins, J. Seabra, Mech. Mach. Theory **166** (2021)
10. L. Steinle, A. Lechler, M. Neubauer, A. Verl, Production Engineering **16** (2022)
11. Z. Chen, M. Zeng, A. Fuentes-Aznar, J. Mech. Des. **142** (2020)
12. M. Duchemin, V. Collee, SAE Int J Engines **9** (2016)
13. D Marano, A Piantoni, L Tabaglio, M Lucchi, M. Barbieri, F. Pellicano *First World congress on condition monitoring* (2017)
14. C. Zhou, X. Dong, H. Wang, Z. Liu, J. Brazilian Soc. Mech. Sci. & Eng. **44** (2022)
15. J. Larrañaga, I. Ulacia, A. Iñurritegui, A. Arana, J. German, J. Elizegi, *AGMA FTM* (2018)
16. F.L. Litvin, A. Fuentes, I. Gonzalez-Perez, L. Carvenali, K. Kawasaki, R.F. Handschuh, Comp. Meth. in App. Mech. and Eng. **192** (2003)
17. P. Dumitrache, Mechanical Engineering **17** (2012)
18. Abaqus theory manual.
19. A. Iñurritegui, A. Arana, M. Hernandez, J. Elizegi, I. Ulacia, J. Larrañaga, *XXII CNIM.* (2018)
20. M.B. Sánchez, M. Pleguezuelos, J.I. Pedrero, Mech. Mach. Theory **139** (2019)
21. M.B. Sánchez, M. Pleguezuelos, J.I. Pedrero, Mech. Mach. Theory 133 (2019)
22. M.B. Sánchez, M. Pleguezuelos, J.I. Pedrero, Meccanica **48** (2013)